

## Dual Role of Lys206–Lys296 Interaction in Human Transferrin N-Lobe: Iron-Release Trigger and Anion-Binding Site<sup>†</sup>

Qing-Yu He,<sup>\*,‡</sup> Anne B. Mason,<sup>‡</sup> Beatrice M. Tam,<sup>§</sup> Ross T. A. MacGillivray,<sup>§</sup> and Robert C. Woodworth<sup>‡</sup>

Department of Biochemistry, College of Medicine, University of Vermont, Burlington, Vermont 05405, and Department of Biochemistry and Molecular Biology, University of British Columbia, Vancouver, BC V6T 1Z3, Canada

Received January 20, 1999; Revised Manuscript Received April 1, 1999

**ABSTRACT:** The unique structural feature of the dilysine (Lys206–Lys296) pair in the transferrin N-lobe (hTF/2N) has been postulated to serve a special function in the release of iron from the protein. These two lysines, which are located in opposite domains, hydrogen bond to each other in the iron-containing hTF/2N at neutral pH but are far apart in the apo-form of the protein. It has been proposed that charge repulsion resulting from the protonation of the dilysines at lower pH may be the trigger to open the cleft and facilitate iron release. The fact that the dilysine pair is positively charged and resides in a location close to the metal-binding center has also led to the suggestion that the dilysine pair is an anion-binding site for chelators. The present report provides comprehensive evidence to confirm that the dilysine pair plays this dual role in modulating release of iron. When either of the lysines is mutated to glutamate or glutamine or when both are mutated to glutamate, release of iron is much slower compared to the wild-type protein. This is due to the fact that the driving force for cleft opening is absent in the mutants or is converted to a lock-like interaction (in the case of the K206E and K296E mutants). Direct titration of the apo-proteins with anions as well as anion-dependent iron release studies show that the dilysine pair is part of an active anion-binding site which exists with the Lys296–Tyr188 interaction as a core. At this site, Lys296 serves as the primary anion-binding residue and Tyr188 is the main reporter for electronic spectral change, with smaller contributions from Lys206, Tyr85, and Tyr95. In iron-loaded hTF/2N, anion binding becomes invisible as monitored by UV–vis difference spectra since the spectral reporters Tyr188 and Tyr95 are bound to iron. Our data strongly support the hypothesis that the apo-hTF/2N exists in equilibrium between the open and closed conformations, because only in the closed form is Lys296 in direct contact with Tyr188. The current findings bring together observations, ideas, and experimental data from a large number of previous studies and shed further light on the detailed mechanism of iron release from the transferrin N-lobe. In iron-containing hTF/2N, Lys296 may still function as a target to introduce an anion (or a chelator) near to the iron-binding center. When the pH is lowered, the protonation of carbonate (synergistic anion for metal binding) and then the dilysine pair form the driving force to loosen the cleft, exposing iron; the nearby anion (or chelator) then binds to the iron and releases it from the protein.

Human serum transferrin (~80 kDa) is one of a group iron-binding and -transport proteins which include lactoferrin and ovotransferrin (1–3). Transferrin binds iron in the ferric form in plasma at neutral pH and transports it into cells where it is released in the acidic endosomal environment. The precise mechanism of iron binding and delivery by transferrin in vivo remains unknown and has been the subject of extensive research. In contrast, the structure of various transferrins has been studied in detail by X-ray crystallography (4–8). A transferrin molecule consists of a single

polypeptide chain that folds into two similar halves, termed the N- and C-lobes, each containing an iron-binding site. The two lobes can further be divided into four domains, the NI and NII domains for the N-lobe and the CI and CII domains for the C-lobe. Iron is held in the binding cleft formed by each pair of domains by coordination to four amino acid residues; one histidine, two tyrosines, and one aspartate and two oxygen atoms from the obligate synergistic anion, carbonate. The same arrangement of binding ligands is found at the functional metal-binding sites in the N- and C-lobes of all transferrins.

In the human transferrin N-lobe (hTF/2N), the binding ligands are Asp 63, Tyr95, Tyr188, and His249. When iron is released, the two domains of hTF/2N rotate apart 63° to assume an open conformation (8, 9). Besides binding iron, the protein can also accommodate other metal ions of similar ionic radii and charge. A recent structural study has confirmed that there is an extensive hydrogen bond network, the so-called “second shell” surrounding the iron-binding site

<sup>†</sup> This work was supported by USPHS Grant R01 DK 21739 (to R.C.W.) from the National Institute of Diabetes and Digestive and Kidney Diseases and by shared instrumentation Grant S10 RR12926-01 (to R.C.W.) from the National Center for Research Resources. Q.-Y.H. was supported by the Postdoctoral Fellowship from the American Heart Association, ME/NH/VT Affiliate.

\* To whom correspondence should be addressed. Phone: (802) 656-0343. Fax: (802) 862-8229. E-mail: qhe@zoo.uvm.edu.

<sup>‡</sup> University of Vermont.

<sup>§</sup> University of British Columbia.

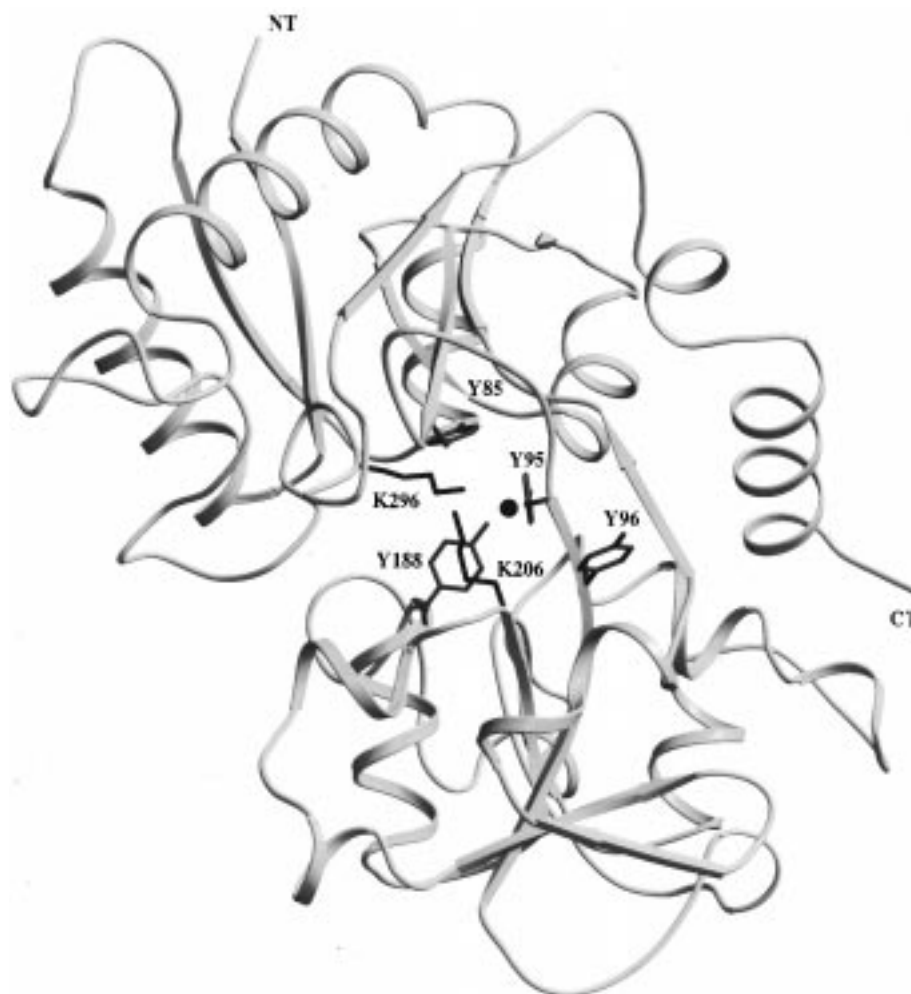


FIGURE 1: The position of the dilysine pair (K206 and K296) and the four tyrosine residues in the vicinity of the metal-binding site of Fe(III)-hTF/2N (8). The N-terminus (NT) and C-terminus (CT) of hTF/2N are labeled. The iron atom is shown as a black sphere at the bottom of the cleft, adjacent to the two tyrosine ligands (Y188 and Y95). The other ligands (D63, H249, and the carbonate anion) are not shown. The figure was generated using the computer programs Molscript (31) and Raster3D (32).

(8). This network helps to hold the ligands in the proper position and stabilizes the metal-binding center. The residues in the H-bond network include Gly65, Glu83, Tyr85, Arg124, Lys206, Ser248, and Lys296. Mutating any of them to give other side chains may be expected to affect the iron binding properties of the protein.

Two members of the second shell, Lys206 and Lys296, reside in opposite domains but are linked to each other by hydrogen bonds in iron-loaded hTF/2N (Figure 1). Analysis of this structural feature in the ovotransferrin and the human transferrin N-lobes led to the term “dilysine trigger,” which was proposed to modulate the opening and closing of the cleft at different pHs (10). In addition, this same dilysine pair has been implicated in a kinetically significant anion binding (KISAB)<sup>1</sup> site for iron release due to its positive charge and location near the metal-binding center (3, 11–13) and in divalent anion binding by the apo-protein (14). In the present study, these two lysine residues have been

mutated to either glutamate (K206E and K296E) or glutamine (K206Q and K296Q), and the double mutant K206E/K296E has been produced. The mutations were made to test the effect of charge on the particular lysine residue without a radical change in size. The metal binding and release behaviors of the resulting mutants are compared to those for the recombinant wild-type hTF/2N. As detailed by Li et al., the recombinant wild-type hTF/2N effectively mimics the N-lobe in full-length transferrin in vitro in terms of its iron binding properties (15). The present report shows that the Lys206–Lys296 interaction is a critical structural feature in iron release and also serves as an anion-binding site. This dual role for the dilysine pair is an important modulating mechanism for the release of iron from the N-lobe of human transferrin.

## MATERIALS AND METHODS

**Materials.** Chemicals were of reagent grade. Stock solutions of Hepes, Mes, and other buffers were prepared by dissolving the anhydrous salts in Milli-Q (Millipore) purified water and adjusting the pH to desired values with 1 N NaOH or HCl. Standard solutions of copper(II) (10 000  $\mu\text{g/mL}$ ) and iron(II) (1000  $\mu\text{g/mL}$ ) in 5%  $\text{HNO}_3$  were obtained from Johnson Matthey. Cupric chloride came from J. T. Baker

<sup>1</sup> Abbreviations: hTF/2N, recombinant N-lobe of human transferrin comprising residues 1–337; mutants of hTF/2N are designated by the wild-type amino acid residue, the sequence number and the amino acid to which the residue was mutated; BHK, baby hamster kidney cells; NTA, nitrilotriacetate; EDTA, ethylenediaminetetraacetate; Tiron, 4,5-dihydroxy-1,3-benzenedisulfonate; KISAB, kinetically significant anion binding.

Chemical Co., 4,5-dihydroxy-1,3-benzenedisulfonate (Tiron) from Fisher Scientific Co., ethylenediaminetetraacetate (EDTA) from Mann Research Laboratories, Inc., and nitrilotriacetate (NTA) from Sigma. Centricon 10 microconcentrators were from Amicon. Tiron and EDTA stock solutions were prepared by dissolving these chelators in the appropriate buffers and adjusting the pH to the desired values with 1 M NaOH.

**Molecular Biology.** Mutation of each of the two lysines to alternative amino acids was carried out by using a polymerase chain reaction (PCR) based mutagenesis procedure (16). PCR products of the mutagenesis reactions were ligated into Bluescript SK containing the hTF/2N cDNA. The nucleotide sequences of the inserts were determined to confirm the introduction of the specific mutations and the absence of any other mutations. The mutated hTF/2N cDNAs were excised from the Bluescript vector, blunt-ended, and ligated into the *Sma*I site of the pNUT expression vector. Restriction endonuclease mapping was used to confirm the correct orientation (17, 18).

**Expression, Purification, and Preparation of Proteins.** The N-lobe of hTF and the single and double mutants of hTF/2N were expressed by using the pNUT-BHK cell system. Isolation and purification of the recombinant proteins followed the general strategy used previously with a few modifications: after addition of sodium azide (0.02%) and a saturating amount of  $\text{Fe}(\text{NTA})_2$ , the samples were kept frozen until a total of four or five batches had accumulated. These were thawed, pooled, reduced in volume and exchanged into 5 mM Tris-HCl, pH 8.0, using a spiral cartridge concentrator. Purification was achieved by anion-exchange chromatography, specifically, Poros 50 HQ resin in a  $2.6 \times 20$  cm column. Following clarification of the sample by centrifugation at 5900g at 4 °C for 15 min, it was applied to the Poros column using a Pharmacia P-1 pump at a rate of approximately 10 mL/min. Elution from the column involved a single step of 120 mM Tris/HCl, pH 8.0, and collection of 8 mL fractions. All tubes containing pink color were pooled, reduced in volume to  $<10$ , and applied to a Sephacryl S-100 HR column ( $5 \times 80$  cm) equilibrated and run in 0.1 M  $\text{NH}_4\text{HCO}_3$  as described in detail previously (19, 20).

Fe(III)-loaded protein was prepared by adding a slight excess of  $\text{Fe}(\text{NTA})_2$  to a pH 7.4 buffer containing apo- or Fe-unsaturated protein and bicarbonate and then exchanging the sample into 50 mM Hepes using a Centricon 10 microconcentrator (18). The preparation of most apo-protein samples followed the procedure described in detail previously (18). The apo-forms of the K206E and K206Q mutants which bind iron with high affinity were prepared by adding at least a 20-fold excess of EDTA into the buffer solution (pH 4.9) containing the proteins and allowing them to stand at 4 °C for 2 days.

**Electronic Spectra.** UV-vis spectra were recorded on a Cary 219 spectrophotometer under the control of the computer program Olis-219s (On-line Instrument Systems, Inc., Bogart, GA). Hepes buffer (50 mM, pH 7.4) served as the reference for full-range spectra from 250 to 650 nm. Difference spectra were generated by storing the spectrum of the apo-protein as the baseline and subtracting it from the sample spectra.

**Kinetics of Metal Removal.** The kinetics of metal removal from transferrin and the processing of the data were usually

Table 1: Summary of the Spectral Characteristics for Recombinant Wild-Type (WT) and Mutants of Fe-hTF/2N

protein	$\lambda_{\text{max}}$ (nm)	$\lambda_{\text{min}}$ (nm)	$A_{\text{max}}/A_{\text{min}}$	$A_{280}/A_{\text{max}}$
WT <sup>a</sup>	472	410	$1.37 \pm 0.02$	$23.5 \pm 0.1$
K206E	464	402	$1.39 \pm 0.01$	$26.1 \pm 0.2$
K206Q	455	400	$1.38 \pm 0.01$	$26.1 \pm 0.1$
K296E	472	412	$1.37 \pm 0.02$	$26.8 \pm 0.1$
K296Q	470	408	$1.37 \pm 0.01$	$26.7 \pm 0.1$
K206E/K296E	474	412	$1.37 \pm 0.01$	$24.8 \pm 0.2$

<sup>a</sup> From He et al. (22).

carried out by means of the procedure described previously (18, 21, 22). Tiron was used as the chelator for iron removal at pH 7.4 (50 mM Hepes) and EDTA was used as the chelator at pH 6.1 and 5.6 (50 mM Mes). Rate constants for iron removal from the Lys mutants at pH 7.4 were estimated based on a 5 h assay. The data were analyzed with single-exponential functions, giving  $R^2$  values (coefficients of determination) greater than 0.99 in all cases.

For iron release from wild-type Fe-hTF/2N by EDTA at pH 5.6, the kinetics were determined by employing an Olis-RSM 1000 stop-flow spectrophotometer, a new generation of machine with greatly increased sensitivity. One syringe contained protein sample in  $\text{H}_2\text{O}$  ( $A_{280} = 0.5$ ) and a second syringe contained chelator and anion (chloride or sulfate) in Mes buffer (0.1 M, pH 5.6). The spectra were recorded starting 5 ms after mixing. The final concentrations are  $\sim 6.5$   $\mu\text{M}$  protein and 50 mM Mes; the path-length of the cell was 1 cm. The UV-vis absorbance module was used to monitor the spectral change with 472 nm as the central wavelength (357–587 nm full scale) for at least 4 half-lives. The absorbance vs time data were fitted with the software supplied by Olis using the 2D fitting mode. All parameters derived from the fitting were examined to ensure a good fit. The reported data are the average value of at least four assays.

**Anion-Binding Titration.** The anion titrations of apo-protein and the calculation of the binding constants were carried out as previously described (14). Hepes (50 mM) was used for titrations at pH 7.4 and Mes (50 mM) was used for titrations at pH 6.1 and pH 5.6. In each case, the protein concentration was about 13  $\mu\text{M}$ .

## RESULTS

**Electronic Spectra.** Fe(III)-hTF/2N has a characteristic pink color, with maximum ( $\lambda_{\text{max}}$ ) and minimum ( $\lambda_{\text{min}}$ ) absorbances at 472 and 410 nm, respectively, in the UV-vis spectrum. These values combined with the ratios  $A_{\text{max}}/A_{\text{min}}$  and  $A_{280}/A_{\text{max}}$ , reflect the metal-binding properties of the protein and therefore can be regarded as intrinsic spectral parameters. Table 1 lists these parameters for the wild-type hTF/2N and the five lysine mutants. Compared to the wild-type hTF/2N, the mutants K206E and K206Q have a small blue-shift in the  $\lambda_{\text{max}}$  while the  $\lambda_{\text{max}}$  for the K296E and K296Q mutants and the double mutant K206E/K296E are essentially unchanged. All of the mutants have a slightly higher  $A_{280}/A_{\text{max}}$ . These electronic spectral parameters imply that the metal binding sphere in the hTF/2N is not significantly perturbed by the introduction of the mutations.

**Iron Removal at Different pHs.** Iron removal kinetics were determined to assess the effect of the mutations on the iron-



Table 2: Rate Constants,  $k_{\text{obs}}$  ( $\text{min}^{-1}$ ), for Iron Removal from Wild-Type hTF/2N and the Mutants at 25 °C

protein	Fe removal by Tiron <sup>a</sup> (pH 7.4)	Fe removal by EDTA <sup>b</sup> (pH 5.6)
hTF/2N (WT)	$(2.25 \pm 0.09) \times 10^{-2}$	$4.09 \pm 0.16$
K206E	$(6.42 \pm 0.04) \times 10^{-5}$ (2%)	$(1.61 \pm 0.09) \times 10^{-4}$
K206Q	$(8.82 \pm 0.11) \times 10^{-5}$ (3.5%)	$(1.05 \pm 0.03) \times 10^{-2}$
K296E	$(1.28 \pm 0.08) \times 10^{-4}$ (5%)	$(1.49 \pm 0.08) \times 10^{-2}$
K296Q	$(2.04 \pm 0.13) \times 10^{-4}$ (7%)	$(3.75 \pm 0.21) \times 10^{-2}$
K206E/K296E	$(6.11 \pm 0.26) \times 10^{-4}$ (19%)	$(8.98 \pm 0.42) \times 10^{-2}$

<sup>a</sup>  $k$  for hTF/2N is from He et al. (18),  $k$ s for the mutants are estimated based on the data of 5 h assay. Values in parentheses are the percentages of iron removed after 5 h. Hepes = 50 mM, pH 7.4, Tiron = 12 mM.  
<sup>b</sup>  $k$  for K206E is based on the data of 5 h assay. Mes = 50 mM, pH 5.6, EDTA = 4 mM.

binding stability of the protein. The rate constants listed in Table 2 reveal that iron removal from the mutants at neutral pH is extremely slow. On the basis of the data collected over 5 h, only 2–19% of the iron was removed from the mutants.

Iron removal from the lysine mutants at pH 5.6, an approximation of the pH in the acidified endosome, can be measured but is still slow (Table 2). In the case of the K206E mutant, iron is removed from the protein so slowly that a kinetic assay is difficult even at the lower pH. The estimated rate constant for the mutant K206E based on a 5 h assay is  $1.61 \times 10^{-4} \text{ min}^{-1}$ . In contrast, iron is rapidly removed from wild-type hTF/2N at pH 5.6; the rate constant range  $(50\text{--}25000) \times 10^4$  times larger than that found for the mutants. In terms of lability, iron removal from the proteins at both pH 5.6 and 7.4 follows the same order: K206E < K206Q < K296E < K296Q < K206E/K296E  $\ll$  hTF/2N.

**Anion Effect on Iron Removal.** Anion-dependent iron removal kinetics were determined in the presence of chloride. The chloride-dependent iron removal for the K206E mutant has not been performed due to the very slow reaction. Rate constants listed in Table 3 and plotted in Figure 2 show that chloride inhibited iron release from all the mutant proteins and the inhibition occurred in a hyperbolic mode. Iron removal from the mutant K206Q is different from the other mutants. As the concentration of chloride increases from 0 to 500 mM, the K206Q mutant shows less sensitivity than the other mutants to the retarding effect of chloride (Figure 2B). Interestingly, chloride exerts different effects on the iron removal from wild-type hTF/2N at different pH values (Figure 3), as has been reported in our earlier work (21). Chloride-retarded iron removal from hTF/2N at pH 7.4 in a negative hyperbolic mode (Figure 3A) and accelerated the removal at pH 5.6 in a positive hyperbolic mode (Figures 2A and 3C). At pH 6.1, the chloride effect yielded a unique pattern: as the chloride concentration increased, the iron

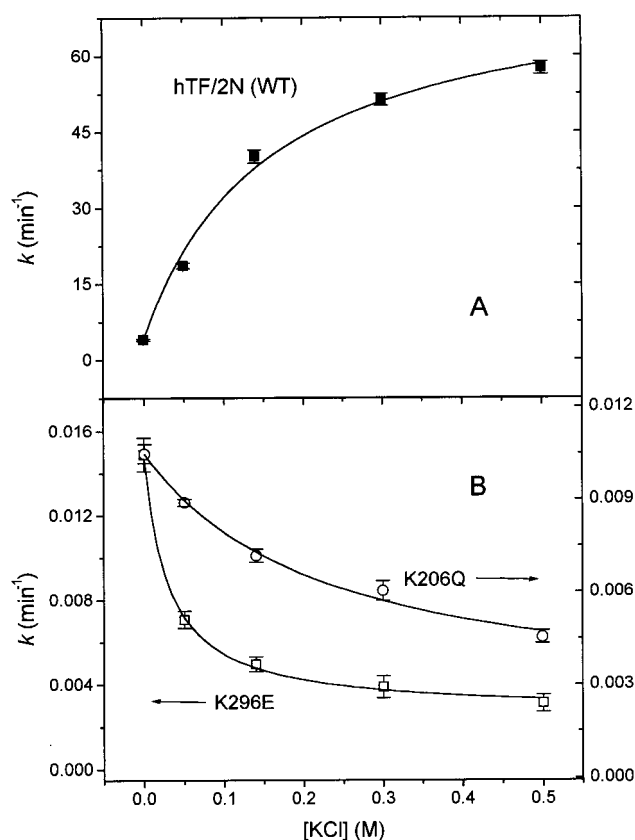


FIGURE 2: Plots of the effect of chloride on iron removal from wild-type hTF/2N and the lysine mutants with EDTA (4 mM). Protein ( $\sim 39 \mu\text{M}$ ), Mes (50 mM), pH 5.6, 25 °C. (A) hTF/2N (WT). (B) K206Q and K296E (K296Q and K206E/K296E have a pattern similar to K296E).

removal rate sharply increased, reaching a maximum point at  $[\text{KCl}] = 0.1 \text{ M}$ , after which the rate slowly decreased (Figure 3B).

The anion-effect on iron removal was also explored using sulfate. Figure 3 shows the comparison for the chloride and sulfate dependent iron removal from wild-type hTF/2N. It is clear that sulfate has a greater effect than chloride both in retarding iron removal at pH 7.4 and in accelerating the removal at pH 5.6 (Figure 3, panels A and C). At pH 6.1, sulfate exerted its influence in a similar mode to that of chloride but with more extreme results (Figure 3B). Sulfate induces a dramatic increase in the iron-removal rate for hTF/2N at low concentration and then drops off sharply with a maximum point at  $[\text{K}_2\text{SO}_4] = 25 \text{ mM}$ . The effect of sulfate on iron removal from the mutants was investigated using the K296Q mutant as a representative sample for comparison with wild-type hTF/2N. In contrast to wild-type hTF/2N, the K296Q mutant lacks the Lys296 residue which is mainly

Table 3: Rate Constants,  $k_{\text{obs}}$  ( $\text{min}^{-1}$ ), for Iron Removal from the Mutants of hTF/2N at Various KCl Concentrations<sup>a</sup>

	KCl (mM)				
	0	50	140	300	500
hTF/2N (WT)	$4.1 \pm 0.16$	$18.7 \pm 0.59$	$40.2 \pm 1.28$	$51.4 \pm 1.16$	$57.5 \pm 1.29$
K206Q	$(1.05 \pm 0.03) \times 10^{-2}$	$(8.91 \pm 0.11) \times 10^{-3}$	$(7.18 \pm 0.21) \times 10^{-3}$	$(6.05 \pm 0.32) \times 10^{-3}$	$(4.55 \pm 0.20) \times 10^{-3}$
K296E	$(1.49 \pm 0.08) \times 10^{-2}$	$(7.09 \pm 0.41) \times 10^{-3}$	$(4.98 \pm 0.36) \times 10^{-3}$	$(3.89 \pm 0.52) \times 10^{-3}$	$(3.11 \pm 0.41) \times 10^{-3}$
K296Q	$(3.75 \pm 0.21) \times 10^{-2}$	$(2.60 \pm 0.22) \times 10^{-2}$	$(1.60 \pm 0.10) \times 10^{-2}$	$(1.10 \pm 0.06) \times 10^{-2}$	$(7.41 \pm 0.31) \times 10^{-3}$
K206E/K296E	$(8.99 \pm 0.43) \times 10^{-2}$	$(6.28 \pm 0.28) \times 10^{-2}$	$(5.24 \pm 0.04) \times 10^{-2}$	$(4.86 \pm 0.18) \times 10^{-2}$	$(4.91 \pm 0.09) \times 10^{-2}$

<sup>a</sup> The chloride-dependent iron removal for the K206E mutant has not been performed due to the very slow reaction. Mes (50 mM), pH 5.60, [EDTA] = 4.0 mM, 25 °C.

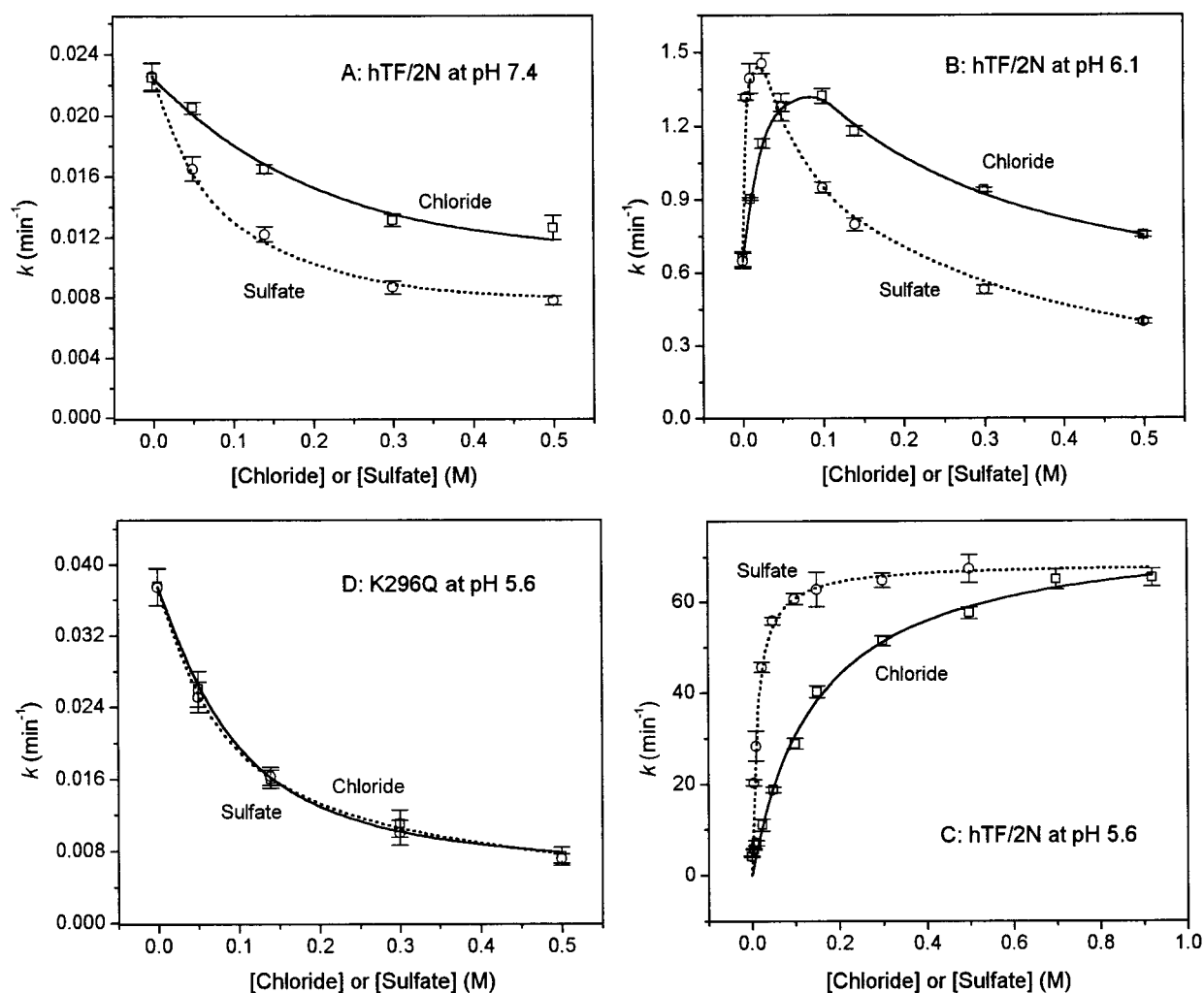


FIGURE 3: Comparison of different anion effects on iron removal from wild-type and mutant proteins. Tiron (12 mM) was the chelator for iron removal at pH 7.4 (Hepes 50 mM), and EDTA (4 mM) was the chelator at pH 6.1 and 5.6 (Mes 50 mM), 25 °C. Open squares for chloride and open circles for sulfate. (A) Wild-type hTF/2N at pH 7.4. (B) Wild-type hTF/2N at pH 6.1. (C) Wild-type hTF/2N at pH 5.6 and (D) K296Q at pH 5.6.

responsible for anion binding (see Discussion). The plot in Figure 3D shows that there is essentially no difference between sulfate and chloride with respect to the anion effect on iron removal from the Fe–K296Q mutant.

**Anion Binding.** Anion binding studies were performed for the wild-type and the lysine mutant apo-proteins under the same conditions used for determining the iron removal kinetics. Figure 4 gives the UV–vis difference spectra obtained after addition of 2 mM sulfate to a solution of apo-protein at pH 7.4. The wild-type hTF/2N exhibited the typical electronic spectral absorption: two negative absorbance bands at 245 and 298 nm and a small positive band at around 276 nm (14, 23, 24). The K206Q mutant has a similar difference absorption spectrum although the absorptivity is lower; all the remaining lysine mutants including K206E give no observable absorbance under the identical conditions. The calculated values of binding constants are  $5.84 \times 10^3 \text{ M}^{-1}$  for hTF/2N (WT),  $1.67 \times 10^3 \text{ M}^{-1}$  for K206Q, and zero for the other lysine mutants (Table 4); these results are consistent with the earlier work in this laboratory (14). Chloride binding to the apo-proteins has a similar profile but is much weaker. The estimated binding constants are 38 and  $12 \text{ M}^{-1}$ , respectively, for the wild-type hTF/2N and the K206Q mutant. The value for the wild-type protein is consistent with

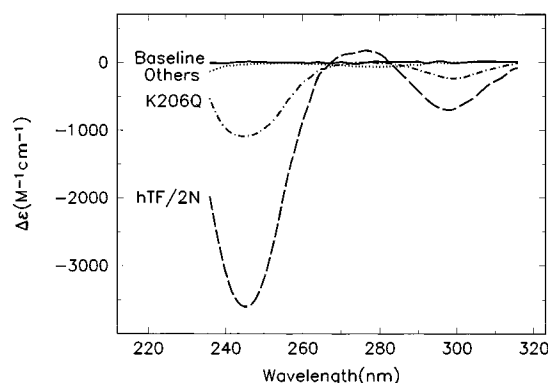


FIGURE 4: UV–vis difference spectra for sulfate (2 mM) titration to apo-proteins (~13 μM). Hepes (50 mM), pH 7.4, 25 °C. Titration with chloride generated a similar profile but with less absorptivity.

the value reported for the N-lobe in full-length transferrin (24). At the lower pH 5.6, the binding of the two anions to hTF/2N was also stronger than the binding to the K206Q mutant and no detectable binding to other lysine mutants was observed.

To explore the structural basis for detection of anion binding, titration with sulfate was carried out for four tyrosine mutants, Y85F, Y95F, Y96F, and Y188F. The resulting

Table 4: Sulfate Binding to Apo Wild-Type and Mutant hTF/2N Proteins<sup>a</sup>

protein	$\Delta\epsilon_{\max} \times 10^{-3}$ (M <sup>-1</sup> cm <sup>-1</sup> )	$K (1/K_d) \times 10^{-3}$ (M <sup>-1</sup> )
hTF/2N (WT)	5.17	5.84
K206Q	2.04	1.67
Y85F	6.27	8.84
Y95F	3.15	7.86
Y96F	5.37	5.82
Y188F	1.67	1.63

<sup>a</sup> Hepes (50mM), pH 7.4, 25 °C, [protein]  $\approx$  13  $\mu$ M. The calculation of the binding constants was carried out as previously described using the equation,  $\Delta\epsilon_{\text{cal}} = \Delta\epsilon_{\max} \times [X]/(K_d + [X])$ , where X is sulfate anion (14).

maximum absorptivity ( $\Delta\epsilon_{\max}$ ) and binding constants ( $K$ ) are summarized in Table 4. Compared to the wild-type hTF/2N, mutant Y96F has similar absorptivity  $\Delta\epsilon_{\max}$ , and binding constant  $K$ , mutant Y95F has a smaller  $\Delta\epsilon_{\max}$  and a larger  $K$ , while mutant Y85F shows a slightly larger  $\Delta\epsilon_{\max}$  and a much larger  $K$ . Interestingly, both  $\Delta\epsilon_{\max}$  and  $K$  values for mutant Y188F are small, less than one-third of those for the wild-type hTF/2N, implying a significant contribution from the residue Tyr188 to the anion binding.

## DISCUSSION

*Lys206–Lys296 Pair Is a Critical Iron Release Trigger.* Lys206 and 296 are two residues in the second-shell hydrogen-bond network surrounding the metal-binding center of the transferrin N-lobe and located on opposite domains of the N-lobe (8, 25). In many iron-containing transferrins, these two lysines are linked by hydrogen bonds (the distance between the two lysines is 2.3 Å in ovotransferrin and 3.1 Å in human transferrin). In the apo-proteins, these two lysines are far apart (9.0 Å) apparently as a result of cleft opening when the two domains pivot away from each other (9, 25). The existence of this structural feature led to the proposal of a “dilysine trigger”; at the low pH of the acidic endosome, these two lysines from opposite domains would be protonated, the resulting positive charges forming a driving force to open the cleft of the protein, exposing the iron and facilitating its release (10). Accordingly, in the absence of the dilysine trigger, proteins such as lactoferrin and the C-lobe of transferrin would hold iron more tightly, making iron removal more difficult (3). The findings from the present study support this hypothesis. Mutating either K206 or K296 in the dilysine pair to glutamate or glutamine led to very slow iron removal (Table 2). Since the mutations do not perturb the metal-binding sphere of the protein as reflected by the similar electronic spectral characteristics between the mutants and wild-type hTF/2N, the extremely tight iron binding in the mutants is clearly due to the mutations which influence the interaction of the dilysine pair.

The difference in the rates of iron removal  $K206E < K206Q < K296E < K296Q < K206E/K296E \ll$  hTF/2N implies that these two lysines are not equivalent in the dilysine trigger. Mutation of Lys206 has a more pronounced impact than mutation of Lys296. Whenever either of the lysines is substituted by a glutamate, the negative charge thus introduced could allow interaction with the positive charge from the remaining lysine to form a salt bridge. The driving force for cleft opening in the original dilysine pair

would then be converted to a lock-like interaction. This may explain why the rate of iron removal from the K206E and K296E mutants is dramatically slower. Mutating either of the lysines to a glutamine, a neutral residue, also appears to perturb the dilysine trigger. Because the glutamine cannot be protonated to provide a positive charge, the driving force for cleft opening is eliminated. The crystal structure of the Fe–K206Q mutant protein (not yet finalized) shows that the distance between the K296NZ and the Q206NE2 is less than 3 Å, suggesting that these two side-chain atoms have the potential to form a stabilizing H-bond (A. Yang, Y. Luo, J. Chen, Y. Wang, A. B. Mason, R. C. Woodworth, R. T. A. MacGillivray, G. D. Brayer, and M. E. P. Murphy, unpublished results). This appears to be the reason the K206Q and K296Q mutants have much greater kinetic stability than wild-type hTF/2N but smaller than the corresponding glutamate mutants, K206E and K296E. The double mutant K206E/K296E allowed introduction of a “diglutamate trigger”. However, as might be expected, the diglutamate interaction is not as strong as the dilysine interaction, especially at low pH. The double mutant therefore still holds iron more tightly than wild-type hTF/2N but more loosely than the single point mutants.

*Lys206–Lys296 Pair Is an Active Anion-Binding Site.* It has been suggested that the dilysine pair may be an anion-binding site (3, 11–13). The titration of the lysine mutants and the wild-type apo-hTF/2N with sulfate presented in Figure 4 indicates that Lys296 is likely a key anion-binding residue or a major part of a combined site for anion binding. When the apo-proteins were titrated with sulfate or chloride, wild-type hTF/2N displayed a typical anion-binding spectrum (14, 24), whereas the K296E, K296Q, and K206E/K296E mutants gave no specific response. This lack of reactivity appears to be due to the absence of Lys296. In addition, the K206E mutant also shows no binding of anion, probably due to the involvement of Lys296 in the mutant in a salt bond with the negative side chain of Glu 206. For the K206Q mutant, the anion binding takes place but is weaker. This implies that the Lys206 is a minor contributor to the anion-binding site; without it (in the K206Q mutant), the anion-binding ability of the protein is impaired (see below). This observation provides support for the hypothesis that in the apo-N-lobe of transferrin the two domains are sampling open and closed conformations (26), since only if the two domains are in proximity could the Glu or Gln 206 in the K206 mutants affect the anion-binding of Lys296 by interacting with it (see Figure 1). We reiterate that in the open conformation the two lysines are 9 Å apart.

The dilysine anion-binding site appears to have a significant effect on the kinetics of iron release. Sulfate has a greater effect than chloride on iron removal from wild-type hTF/2N at both neutral and acidic pH, whereas sulfate and chloride show no difference in retarding iron removal from the K296Q mutant (Figure 3). This finding corresponds perfectly with the observation that sulfate binds hTF/2N more strongly than chloride and neither sulfate nor chloride binds the K296Q mutant apo-protein (in the  $\Delta A_{245}$  assay).

Our previous studies found that, in wild-type hTF/2N, chloride retards iron release at high pH and accelerates iron release at low pH with an isotropic point at pH 6.26 (21). The results presented in Figure 3, panels A–C, reflect the anion-dependent iron removal at pH 7.4–5.6, which appar-

ently corresponds to the protonation behavior and thus the anion-binding ability of the dilysine pair at the different pH values. The double phase for the iron removal at pH 6.1 (a pH slightly lower than the isotropic point) is especially important in elucidating the anion effect. As shown in Figure 3B, at low anion concentration prior to saturation of the anion-binding site (the maximum point at  $[KCl] = 0.1$  M), chloride assists the chelator in removal of iron; after this point, the large amount of chloride gradually dominates the competition with chelator for the anion-binding site, K206–K296, so that a retarding trend is observed. Iron removal in the presence of sulfate heightens the effect as might be predicted because sulfate binds more avidly to the anion-binding site. Taken together, the pH and salt-dependent phenomena suggest that the salt-dependent mechanism changes in response to the protonation of a critical residue(s) in the protein and that the two effects are interacting. This situation is reminiscent of the site preference in holo-hTF as functions of pH and salt concentration (27).

**Dilysine Pair Is Not the Only Anion-Binding Site.** The existence of anion-binding site(s) other than the dilysine pair is likely. This is illustrated by the fact that iron removal from the lysine mutants still shows some sensitivity to inorganic anions (Table 3 and Figure 2), although ionic strength effects might be a contributing factor to the observed influence of anions. In the case of apo-hTF/2N, direct evidence for anion binding to Lys296 can be observed by UV–vis difference spectroscopy. However, the fact that there was no UV–vis spectral change after addition of anions to iron-loaded hTF/2N (23, 28) does not necessarily exclude anion binding to the protein. Other possible anion-binding sites involving different residues may be silent in the electronic spectra but may be monitored by other techniques. Grady et al. have demonstrated chloride binding to hTF/2N and various single-point mutants by means of EPR spectroscopy, in which all of the iron-containing proteins showed sensitivity to anion binding (29). Of great interest is the fact that chloride binding to the Fe-K296E mutant displayed a totally different profile from the chloride binding to wild-type hTF/2N. These results reinforce the present argument that anion-binding site(s) other than Lys296 may exist but that Lys296 is an important residue in the anion-binding site.

**Other Residues in Addition to the Dilysine Augment the Anion-Binding Site.** The anion-binding site of Lys206–Lys296 appears to contain other residue(s). Since the UV–vis difference spectra associated with the dilysine binding site report the interaction between anion and the phenolic oxygen of tyrosine side chain(s), other residue(s) comprising the anion-binding site should involve tyrosine(s) in the vicinity of Lys296 (Figure 1). Anion-binding titration of the tyrosine mutants, Y85F, Y95F, Y96F, and Y188F, where the four tyrosines were individually replaced by mutation to phenylalanine (22, 25), confirmed that all of these tyrosine residues (except Tyr96) play a role in reporting anion binding (Table 4). Since Tyr96 is not bound to any functional residue, it is reasonable that mutation at Tyr96 has no effect on the binding of anion to the protein. Our earlier work showed that the Y96F mutant has identical metal-binding behavior with the wild-type hTF/2N (22). In contrast, Tyr95 and Tyr188 are metal-binding ligands. Both Tyr85 and Tyr188 are hydrogen bonded to Lys296 in iron-loaded hTF/2N (8). In sharp contrast, none of these three tyrosine residues (Y85,

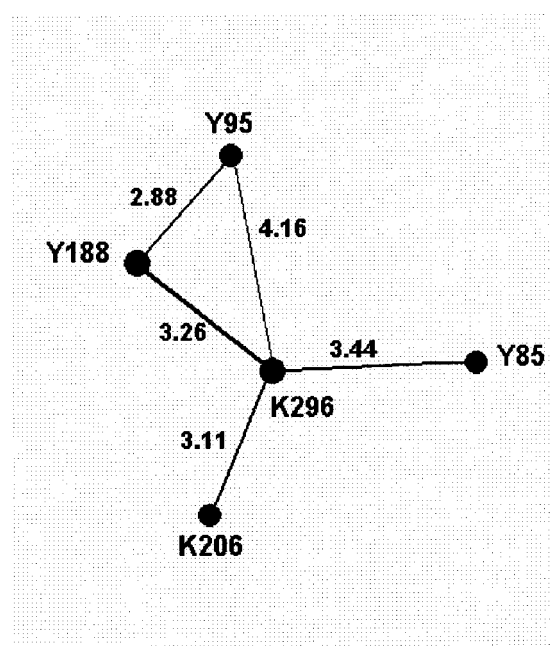


FIGURE 5: A schematic representation of the dilysine anion-binding site. The distances between the residues were taken from their positions in the iron-loaded hTF/2N protein (8). In apo-hTF/2N, only Lys206 and Tyr188 are linked together.

Y95, and Y188) has any connection with Lys296 in the apo-form of hTF/2N (9). Clearly, interaction of the three Tyr residues with the Lys296 site can only be explained if the protein is in the “closed” conformation where these tyrosine side chains are linked with Lys296 in the second shell network (8). It can be assumed that apo-hTF/2N occasionally forms a closed conformation in which the residues Lys296 and Tyr188 make up the core of a combined anion-binding site with Lys296 as a primary anion-binding residue and Tyr188 as a major reporting residue of spectral change (Figure 5).

Other functional residues in the proximity, Lys206, Tyr85, and Tyr95, serve as minor components for the binding site, of which Lys206 assists Lys296 in binding anion and Tyr95 assists Tyr188 in reporting spectral change (Figure 5). It is therefore no surprise that the mutant lacking Tyr188 (Y188F) shows weak response to anion binding (small  $\Delta\epsilon_{\max}$ ) and low binding affinity (Table 4). Also, it is clear that mutation of Tyr95 influences the anion binding of the protein. The apparent large anion-binding constant for the mutant Y85F suggests that the disconnection of Tyr85–Lys296 bonding shifts the position of the anion with respect to Tyr188 and Tyr95, resulting in a higher anion-binding affinity. In fact, a previous report has shown that, under the same conditions, chloride accelerates iron release from the Y85F mutant, in contrast to wild-type hTF/2N where chloride retards iron release (25). This phenomenon is consistent with the unusual anion-binding behavior of the mutant Y85F.

**Dilysine-Modulated Iron Release.** Our current work presents direct and comprehensive evidence of the pronounced effect that mutation of either Lys206 or Lys296 has on iron removal, strongly suggesting that the dilysine trigger is critical for iron release in the N-lobe of human transferrin. In addition, we confirm that the dilysine pair is also a KISAB site. Another anion-binding site (Lys 569) has been identified in the C-lobe of human transferrin (30). It seems clear that



there is more than one KISAB site in hTF/2N, which accounts for the remaining sensitivity of the mutants lacking Lys296 to anions. It is also clear that the dilysine anion-binding site consists of other residues including Tyr188, which is the main reporter for the electronic spectral change upon binding anion, and Tyr85 and Tyr95, which appear to exert their effect through the second shell network. In iron-loaded hTF/2N, Tyr188 and Tyr95 are bound to the metal center, so that anion binding cannot be observed by UV–vis difference spectra. In this case, the combined anion-binding site may still serve as a target to introduce a chelator near to the metal center. A recent paper of the X-ray crystal structure of hTF/2N provides evidence that protonation of the synergistic anion, carbonate, is an important step in iron release (8). When the driving force derived from the protonation of the carbonate and the dilysine pair develops to make the cleft loose enough, the nearby chelator then binds to the metal and releases it from the protein. Obviously, this dual role of the dilysine interaction is extremely important for modulating the release of iron from the N-lobe of transferrin.

## ACKNOWLEDGMENT

We thank Dr. N. Dennis Chasteen of the University of New Hampshire for his helpful comments and suggestions on the manuscript.

## REFERENCES

- Griffiths, E. (1987) in *Iron and Infection* (Bullen, J. J., and Griffiths, E., Eds.) pp 1–25, John Wiley & Sons, Chichester.
- Chasteen, N. D., and Woodworth, R. C. (1990) in *Iron Transport and Storage* (Ponka, P., Schulman, H. M., and Woodworth, R. C., Eds.) pp 67–79, CRC Press, Boca Raton, FL.
- Baker, E. N. (1994) *Adv. Inorg. Chem.* 41, 389–463.
- Anderson, B. F., Baker, H. M., Dodson, E. J., Norris, G. E., Rumball, S. V., Waters, J. M., and Baker, E. N. (1987) *Proc. Natl. Acad. Sci. U.S.A.* 84, 1769–1773.
- Bailey, S., Evans, R. W., Garratt, R. C., Gorinsky, B., Hasnain, S. S., Horsburgh, C., Jhoti, H., Lindley, P. F., Mydin, A., Sarra, R., and Watson, J. L. (1988) *Biochemistry* 27, 5804–5812.
- Kurokawa, H., Mikami, B., and Hirose, M. (1995) *J. Mol. Biol.* 254, 196–207.
- Zuccola, H. J. (1993) *The crystal structure of monoferric human serum transferrin*, Thesis/Dissertation, Georgia Institute of Technology, Atlanta, GA.
- MacGillivray, R. T. A., Moore, S. A., Chen, J., Anderson, B. F., Baker, H., Luo, Y., Bewley, M., Smith, C. A., Murphy, M. E. P., Wang, Y., Mason, A. B., Woodworth, R. C., Brayer, G. D., and Baker, E. N. (1998) *Biochemistry* 37, 7919–7928.
- Jeffrey, P. D., Bewley, M. C., MacGillivray, R. T. A., Mason, A. B., Woodworth, R. C., and Baker, E. N. (1998) *Biochemistry* 37, 13978–13986.
- Dewan, J. C., Mikami, B., Hirose, M., and Sacchettini, J. C. (1993) *Biochemistry* 32, 11963–11968.
- Baker, E. N. and Lindley, P. F. (1992) *J. Inorg. Biochem.* 47, 147–160.
- Egan, T. J., Ross, D. C., and Purves, L. R. (1994) *S. Afr. J. Sci.* 90, 539–543.
- Lindley, P. F., Bajaj, M., Evans, R. W., Garratt, R. C., Hasnain, S. S., Jhoti, H., Kuser, P., Neu, M., Patel, K., Sarra, R., Strange, R., and Walton, A. (1993) *Acta Crystallogr., Sect. D* 49, 292–304.
- Cheng, Y. G., Mason, A. B., and Woodworth, R. C. (1995) *Biochemistry* 34, 14879–14884.
- Li, Y., Harris, W. R., Maxwell, A., MacGillivray, R. T. A., and Brown, T. (1998) *Biochemistry* 37, 14157–14166.
- Nelson, R. M., and Long, G. L. (1989) *Anal. Biochem.* 180, 147–151.
- Funk, W. D., MacGillivray, R. T. A., Mason, A. B., Brown, S. A., and Woodworth, R. C. (1990) *Biochemistry* 29, 1654–1660.
- He, Q.-Y., Mason, A. B., Woodworth, R. C., Tam, B. M., Wadsworth, T., and MacGillivray, R. T. A. (1997) *Biochemistry* 36, 5522–5528.
- Woodworth, R. C., Mason, A. B., Funk, W. D., and MacGillivray, R. T. A. (1991) *Biochemistry* 30, 10824–10829.
- Mason, A. B., Funk, W. D., MacGillivray, R. T. A., and Woodworth, R. C. (1991) *Protein Expression Purif.* 2, 214–220.
- He, Q.-Y., Mason, A. B., and Woodworth, R. C. (1997) *Biochem. J.* 328, 439–445.
- He, Q.-Y., Mason, A. B., Woodworth, R. C., Tam, B. M., MacGillivray, R. T. A., Grady, J. K., and Chasteen, N. D. (1997) *Biochemistry* 36, 14853–14860.
- Harris, W. R. (1985) *Biochemistry* 24, 7412–7418.
- Harris, W. R., Cafferty, A. M., Abdollahi, S., and Trankler, K. (1998) *Biochim. Biophys. Acta* 1383, 197–210.
- He, Q.-Y., Mason, A. B., Woodworth, R. C., Tam, B. M., MacGillivray, R. T. A., Grady, J. K., and Chasteen, N. D. (1998) *J. Biol. Chem.* 273, 17018–17024.
- Gerstein, M., Anderson, B. F., Norris, G. E., Baker, E. N., Lesk, A. M., and Chothia, C. (1993) *J. Mol. Biol.* 234, 357–372.
- Chasteen, N. D., and Williams, J. (1981) *Biochem. J.* 193, 717–727.
- Foley, A. A., and Bates, G. W. (1988) *Biochim. Biophys. Acta* 965, 154–162.
- Grady, J. K., Mason, A. B., Woodworth, R. C., and Chasteen, N. D. (1995) *Biochem. J.* 309, 403–410.
- Zak, O., Tam, B., MacGillivray, R. T., and Aisen, P. (1997) *Biochemistry* 36, 11036–11043.
- Kraulis, P. (1991) *J. Appl. Crystallogr.* 24, 946–950.
- Merritt, E. A., and Murphy, M. E. P. (1994) *Acta Crystallogr., Sect. D* 50, 869–873.

BI990134T